Mass Dependence of the Angular Distribution of Charged-Particle Emission from Crystals: Transition to the Classical Limit

R. E. DE WAMES, W. F. HALL, AND G. W. LEHMAN
Science Center/Aerospace and Systems Group, North American Rockwell Corporation, Thousand Oaks, California

(Received 1 April 1968)

In recent years, the emission of charged particles from crystals has received considerable attention, both experimentally and theoretically. The customary interpretation of the emission partterns has been derived from classical mechanics, which predicts patterns very close to those observed for heavy charged particles (protons, α particles) but only qualitatively similar to those exhibited by electrons and positrons. In the present paper, it is shown that at least one consequence of the classical model, namely, mass independence of the angular distribution at constant energy, is violated dramatically by the quantum-mechanical calculation of the emission pattern. Specifically, the emission patterns for electrons and positrons are shown to differ from the emission patterns for much-higher-mass particles by factors of up to 4 in half-width and intensity. The condition under which the classical limit is regained is that the lattice spacing be large, not compared with the particle de Broglie wavelength, but compared, rather, with $\lambda_p=\hbar/2(m\bar{V})^{1/2}$, where $\bar{V}$ is an average value for the interaction potential inside the unit cell, and m is the particle mass.

I. INTRODUCTION

CHARGED-PARTICLE emission from and penetration into crystals has received considerable attention since the discovery, a few years ago, of marked directional effects in the range of heavy ions in crystals. The qualitative features of this phenomenon have been readily derived from a classical mechanical model in which the incident particle moves in a periodic charge distribution, and it has been repeatedly stated in the literature[1–3] that such a model is very nearly exact at high energy, with no qualification in regard to the mass of the incident particle or the strength of the potential of interaction. It is the purpose of the present paper to show that the quantum-mechanical description of this phenomenon gives results which depart markedly from the classical predictions at small mass and that, for the electron, the emission patterns are only superficially similar to the classical "envelope."

It is easy to show that, according to classical mechanics, the trajectory described by a particle of definite energy moving through some fixed potential field $V(\mathbf{r})$ remains the same if the mass of the particle is changed. Only the time of arrival at each point on the trajectory is altered. Since the classical mechanical model used to derive directional effects in crystals conforms exactly to these conditions, the predicted emission patterns are rigorously independent of particle mass when the energy of emission is held fixed. In the corresponding quantum-mechanical problem, there is a direct dependence of the emission pattern on particle mass, which only disappears as the mass becomes arbitrarily large. Therefore one can use the mass dependence of the calculated emission patterns as a measure of the applicability of the classical results. This is precisely the course that we follow in the present paper.

In Sec. II, we start from the Schrödinger equation which describes the propagation of a charged particle through a periodic potential field, adjoin boundary conditions appropriate to the emission problem, and set forth the techniques that we have used in obtaining solutions. The dependence of the emission pattern on particle mass is illustrated in Sec. III for a screened Coulomb potential of realistic strength and range, with particular attention being paid to the discrepancy between the angular distribution for electrons and that obtained for much-heavier-mass particles. Section IV is devoted to a discussion of the potential dependence of the emitted intensity, which exhibits interesting structure as the mass is varied. Finally, in Sec. V, we discuss the limitations implied by these results on the applicability of the classical model.

II. EMISSION IN A PERIODIC POTENTIAL

The process of particle emission from a crystal occurs in three steps: First, the particle escapes from the atom, then it propagates through the potential field of the crystal, and, finally, it leaves the crystal at a surface with some probability distribution over the outgoing directions. The classical model of this process, which has had considerable success in matching the emission patterns for heavy charged particles, ignores the possibility of energy transfer from the particle to the crystal subsequent to its escape from the atom. The particle is taken to move only under the influence of the periodic potential field of the crystal lattice. It thus behooves us to ask when motion in a periodic potential field can be described by the classical limit. When it cannot, i.e., when quantum effects become important in this simplified version of motion in real crystals, it is certainly

[1] J. Lindhard, Kgl. Danske Videnskab. Selskab, Mat. Fys. Medd. 34, No. 14 (1965), especially pp. 3 and 4.
[2] P. Lervig, J. Lindhard, and V. Nielsen, Nucl. Phys. A96, 481 (1967), especially pp. 481 and 482.
[3] E. Uggerhøj and J. W. Andersen, Can. J. Phys. 46, 543 (1968), especially p. 543.

dangerous to employ the classical results so obtained. Thus we shall consider that the propagation of the particle inside the crystal is governed by the single-particle Schrödinger equation

$$[(-\hbar^2\nabla^2/2m)+U(\mathbf{r})-E]\varphi(\mathbf{r})=0, \quad (1)$$

except in the immediate vicinity of the emitter. In this equation, $U(\mathbf{r})$ is the periodic potential field of the classical model and E is the particle energy at emission.

Near the emitter the external wave function must be matched to the internal wave function corresponding to the state from which the particle escaped. However, if the internal state is taken to be spherically symmetric, the solution to this boundary-value problem far from the emitter is identical with the solution of Eq. (1) with a δ-function source located at the emitter $(\mathbf{r}=\mathbf{r}_e)$:

$$[(-\hbar^2/2m)\nabla^2+U(\mathbf{r})-E]\varphi(\mathbf{r};\mathbf{r}_e)=\delta(\mathbf{r}-\mathbf{r}_e). \quad (2)$$

Outside the crystal the potential vanishes, and at distances large compared with the crystal size, the wave function which matches onto the solution inside the crystal has the form of a spherical wave:

$$\varphi(\mathbf{r};\mathbf{r}_e)\sim f(\theta,\varphi)[\exp(ik_0|\mathbf{r}-\mathbf{r}_e|)/|\mathbf{r}-\mathbf{r}_e|]. \quad (3)$$

Here $\hbar^2k_0^2/2m=E$, and θ and φ are angles defining the direction of $\mathbf{r}-\mathbf{r}_e$ with respect to some set of axes fixed in the crystal.

The problem of determining $f(\theta,\varphi)$, which is proportional to the angular distribution of the emitted particles, can be solved relatively simply by making use of the reciprocity relation

$$\varphi(\mathbf{r};\mathbf{r}_e)=\varphi(\mathbf{r}_e;\mathbf{r}), \quad (4)$$

which follows from Eq. (2) for an arbitrary real potential $U(\mathbf{r})$. This relation, introduced by von Laue[4] to treat inelastic electron scattering in crystals, enables one to find $\varphi(\mathbf{r};\mathbf{r}_e)$ by evaluating the intensity at the emitter site due to a spherical wave emitted from the point $\mathbf{r}$ outside the crystal. When $\mathbf{r}$ is far from the crystal, as in Eq. (3), this wave arrives at the crystal surface as a plane wave directed along $\mathbf{r}_e-\mathbf{r}$. The remaining task, then, is to match this onto the eigensolutions for the periodic potential of Eq. (1) to determine $\varphi(\mathbf{r}_e;\mathbf{r})$ inside the crystal.

It is at this point that the strength of the potential enters forcibly into the problem. Take, first, the extremes: If the crystal potential vanishes, the incident wave reaches the emitter site unaltered; the intensity is unity, independent of the angle of incidence. If, on the other hand, the potential is repulsive and sufficiently strong, no particles will be able to reach the emitter site, and the intensity there will be zero. In between these extremes, when the potential is weak, one sees the intensity depart from unity only at or near the geometrical diffraction resonances known as Bragg peaks; when the potential is strong, these resonances broaden out and blend into one another; motion of the particle into the classically "forbidden" regions diminishes.

These effects are in large measure properties of the individual crystal eigenfunctions onto which the incident wave is tied. Each eigenfunction, because of the periodicity of the potential $U(\mathbf{r})$, will be expressible as a sum over the reciprocal lattice of the crystal:

$$\varphi(\mathbf{r})=\exp(i\mathbf{k}\cdot\mathbf{r})\sum_{\mathbf{h}}u_{\mathbf{h}}\exp(i\mathbf{k}_{\mathbf{h}}\cdot\mathbf{r}), \quad (5)$$

where $\mathbf{k}_{\mathbf{h}}$ is the reciprocal-lattice vector corresponding to the index $\mathbf{h}$. If one expands the potential in a similar fashion,

$$U(\mathbf{r})/E=\sum_{\mathbf{h}}\psi_{\mathbf{h}}\exp(i\mathbf{k}_{\mathbf{h}}\cdot\mathbf{r}), \quad (6)$$

the Schrödinger equation inside the crystal takes the form

$$(2\delta_0+\zeta_{\mathbf{h}})u_{\mathbf{h}}+\sum_{\mathbf{g}}\psi_{\mathbf{h}-\mathbf{g}}u_{\mathbf{g}}=0, \quad (7)$$

where we have written

$$(\hbar^2/2m)k^2-E=2\delta_0E,$$
$$(\hbar^2/2m)(k_{\mathbf{h}}^2+2\mathbf{k}_{\mathbf{h}}\cdot\mathbf{k})=\zeta_{\mathbf{h}}E. \quad (8)$$

Now, angular structure in the intensity is a direct consequence of prominence of some of the coefficients $u_{\mathbf{h}}$ for $\mathbf{h}$ different from zero in the expansion of φ. From Eq. (7), when $\zeta_{\mathbf{h}}$ is small compared with $\psi_{\mathbf{h}}$, then $u_{\mathbf{h}}$ will be comparable in magnitude with u_0; when $\zeta_{\mathbf{h}}$ is large compared with $\psi_{\mathbf{h}}$, then $u_{\mathbf{h}}$ $(\simeq u_0\psi_{\mathbf{h}}/\zeta_{\mathbf{h}})$ will be negligible. Note that, no matter how large one takes k, there will always be an angle (the Bragg angle) at which $\zeta_{\mathbf{h}}=0$, so that for a small but finite crystal potential, one expects angular structure in the intensity only in the immediate vicinity of this angle. On the other hand, if $E\psi_{\mathbf{h}}$ is very large, then $\psi_{\mathbf{h}}/\zeta_{\mathbf{h}}$ will remain appreciable over a wide angular range, even overlapping the Bragg angles for other reciprocal-lattice vectors. Alternatively, from Eq. (8) one sees that if the mass of the incident particle becomes very large, $E\zeta_{\mathbf{h}}$ will remain small over a large angular region. Thus, when either the potential or the mass is sufficiently large, many terms in the sum expression for φ will be of a size comparable with u_0, whatever the direction of $\mathbf{k}$. It is under these conditions that the angular variation of the intensity will be found to approach the classical limit.

The contribution of each eigensolution to the wave function inside the crystal is, of course, determined by the requirement that the logarithmic derivative of $\varphi(\mathbf{r}_e;\mathbf{r})$ be continuous at the crystal surface. However, we shall be interested in particle energies such that $\psi_{\mathbf{h}}$ is small and incident wave vectors $\mathbf{k}_0$ which are directed within a few degrees of the normal to the

[4] M. von Laue, *Materiewellen und ihre Inteferenzen* (Akademische Verlagsgesellschaft, Leipzig, 1948).

crystal surface, and under these conditions one can show that the reflected wave outside the crystal is negligibly small. In this case, the boundary condition can be replaced with the requirement of continuity at the crystal surface

$$\exp(i\mathbf{k}_0\cdot\mathbf{r})=\sum_{j=1}^{N}A_j\exp(i\mathbf{k}^{(j)}\cdot\mathbf{r})\sum_{\mathrm{h}}u_{\mathrm{h}}^{(j)}\times\exp(i\mathbf{k}_{\mathrm{h}}\cdot\mathbf{r})\quad\text{on}\quad\mathbf{r}\cdot\mathbf{n}=0,\tag{9}$$

where $\mathbf{n}$ is the direction of the inward normal to the crystal surface, the superscript j is used to label the eigensolutions of Eq. (7), and N is the number of terms which are kept in the reciprocal-lattice expansion for φ.

One satisfies this boundary condition by choosing

$$\mathbf{k}^{(j)}=\mathbf{k}_0+k_0{}^2\delta_0{}^{(j)}\,\mathbf{n}/\mathbf{k}_0\cdot\mathbf{n}\tag{10}$$

and

$$A_j=\bar{u}_0{}^{(j)},\tag{11}$$

where the bar over u_0 denotes complex conjugation. The intensity at the emitter site can thus be written as

$$\begin{aligned}|\varphi(\mathbf{r}_e;\mathbf{r})|^2&=|\sum_j\bar{u}_0{}^{(j)}\exp(i\mathbf{k}^{(j)}\cdot\mathbf{r})\sum_{\mathrm{h}}u_{\mathrm{h}}{}^{(j)}\times\exp(i\mathbf{k}_{\mathrm{h}}\cdot\mathbf{r})|^2\\&=\sum_j|\bar{u}_0{}^{(j)}\sum_{\mathrm{h}}u_{\mathrm{h}}{}^{(j)}\exp(i\mathbf{k}_{\mathrm{h}}\cdot\mathbf{r})|^2\\&\quad+2\,\mathrm{Re}\sum_{j'>j}[u_0{}^{(j')}\sum_{\mathrm{h}'}\bar{u}_{\mathrm{h}'}{}^{(j')}\exp(-i\mathbf{k}_{\mathrm{h}'}\cdot\mathbf{r})]\\&\quad\times[\bar{u}_0{}^{(j)}\sum_{\mathrm{h}}u_{\mathrm{h}}{}^{(j)}\exp(i\mathbf{k}_{\mathrm{h}}\cdot\mathbf{r})]\\&\quad\times\exp i[k_0{}^2(\delta_0{}^{(j)}-\delta_0{}^{(j')})\,\mathbf{n}\cdot\mathbf{r}/\mathbf{k}_0\cdot\mathbf{n}].\end{aligned}\tag{12}$$

In the second line, the intensity contributed by the cross terms between different eigensolutions has been written separately in order to display their dependence on the distance $(\mathbf{n}\cdot\mathbf{r})$ of the emitter from the crystal surface. Their evaluation, while straightforward, is tedious and adds nothing to the basic character of the solution. In what follows, we shall choose a simple geometry for the crystal and for the incident beam which ensures that these cross terms will oscillate rapidly with emitter depth, so that a collection of emitters spread over a small thickness will yield an average intensity which is just the sum of the diagonal terms in Eq. (12).

The final step in obtaining the emitted intensity is the solution of the eigenvalue problem represented by Eq. (7). As was pointed out earlier, those reciprocal-lattice vectors $\mathbf{k}_{\mathrm{h}}$ for which $\psi_{\mathrm{h}}/\zeta_{\mathrm{h}}$ is sufficiently small can be treated by perturbation, so that the sums in Eq. (7) can be restricted to a finite number of terms and the resulting set can be solved by standard matrix diagonalization techniques. Specifically, we note that the coefficients corresponding to reciprocal-lattice vectors which are not nearly perpendicular to $\mathbf{k}_0$ (i.e., to planes not nearly parallel to $\mathbf{k}_0$) can be neglected when the energy is sufficiently large.

For the simple cubic lattice, this means that one can choose a direction of incidence for $\mathbf{k}_0$ such that $\mathbf{k}_0$ has large projections on two of the three principal reciprocal-lattice directions, so that only coefficients corresponding to the third reciprocal-lattice direction need be retained in Eq. (7). The resulting set of equations is identical with the set that one would obtain if the crystal potential $U(\mathbf{r})$ were replaced with its spatial average over the reciprocal-lattice directions not nearly perpendicular to $\mathbf{k}_0$, so that the effective charge distribution is constant in these directions. Because of the relative simplicity of the mathematics, this effective planar lattice geometry has been chosen to illustrate the mass dependence of the angular variation of the intensity in Sec. III.

A simplification of a different nature becomes possible when $\mathbf{k}_0$ is exactly perpendicular to a principal reciprocal-lattice direction. In this case, each eigensolution of Eq. (7) will be either odd or even with respect to reflection in the appropriate plane, and one can show that only the even eigensolutions can be used in satisfying the boundary conditions at the crystal surface. This reduces by a factor of 2 the number of rows in the matrix which must be diagonalized to obtain the emitted intensity.

An even greater saving is possible when $\mathbf{k}_0$ points

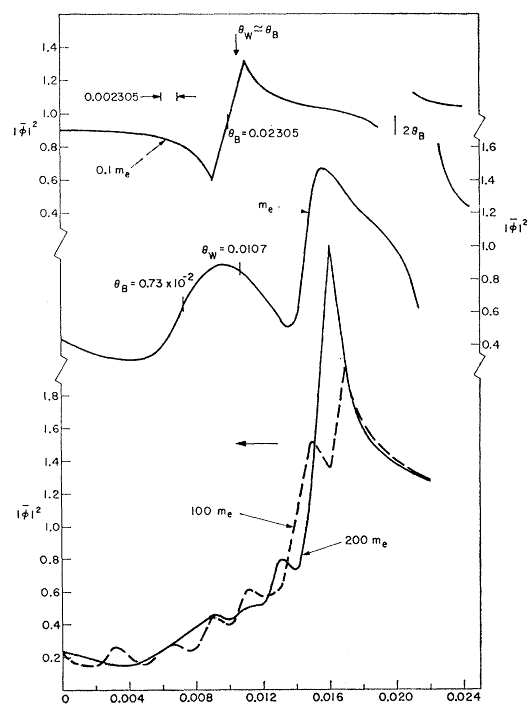

FIG. 1. Mass dependence of the angular variation of the intensity for planar geometry and positive interaction potential. Top curve $m=0.1m_e$, middle curve $m=m_e$, and bottom curves $m=100m_e$ and $200m_e$.

along a reciprocal-lattice direction, and so is perpendicular to both of the other principal directions in the crystal. In this case, for the simple cube, there are eight operations which leave the scattering geometry invariant, and proper use of group theory to classify the eigensolutions of Eq. (7) enables one to reduce the number of rows in the matrix by a factor of 8. A technique for accomplishing this reduction is outlined in the Appendix. This application of symmetry has allowed us to obtain the mass dependence of the intensity along a "string" direction even when several hundred terms had to be retained in the original summation form of Eq. (7).

III. MASS DEPENDENCE OF THE ANGULAR VARIATION OF INTENSITY

The purpose of this section is to illustrate in graphical form the variation of the angular intensity as a function of the mass of the particle for a screened Coulomb potential whose parameters are those associated with the copper lattice. (The calculations are actually made for a simple cubic lattice with a lattice parameter equal to $\frac{1}{2}$ that of the copper lattice. This choice is made in order to correspond to allowed reflections for the fcc lattice.) For simplicity, $\mathbf{k}_0$ is chosen to make a small angle with only one set of planes.

The point here is that there are two distinct regions. For low mass (see topmost curves, Figs. 1 and 2) the angular variation is completely controlled by Bragg angles θ_B and Bragg widths $\Delta\theta_B$. In this situation, the angular variation of the intensity can be calculated

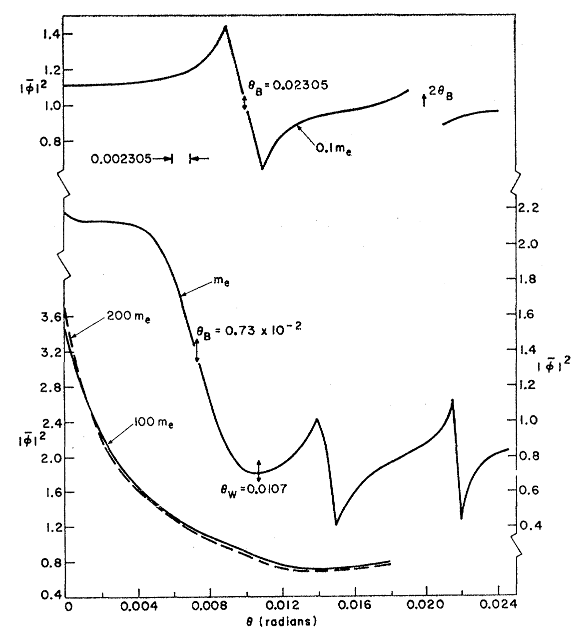

FIG. 2. Mass dependence of the angular variation of the intensity for planar geometry and negative interaction potential. Top curve $m = 0.1m_e$, middle curve $m = m_e$, and bottom curves $m = 100m_e$ and $200m_e$.

using the two-beam theory [i.e., when only two terms are retained in Fourier expansion for $\varphi(\mathbf{r})$]. It can easily be shown from the analytical solution of the two-beam theory[5] that the outer "wing" in the intensity pattern falls at

$$\theta_W = \theta_B + \Delta\theta_B$$
$$= \tfrac{1}{2}[\hbar k_h/(2mE)^{1/2}] + (|V_h|/\hbar k_h)(2m/E)^{1/2}, \quad (13)$$

where V_h is the Fourier transform of the interaction potential evaluated at $\mathbf{k} = \mathbf{k}_h$, and $\mathbf{k}_h$ is the reciprocal-lattice vector for the first-order reflection. The intensity at the origin is slightly below background for the positively charged particle (Fig. 1, top curve) and above background for the negatively charged particle (Fig. 2, top curve). The variation at twice the Bragg angle occurs because of the Bragg reflection of second order.

We note that in the small-mass limit, whether the particle is positively or negatively charged reflects itself in whether we have first a maximum or a minimum in the intensity as we approach the Bragg angle. From Eq. (13) it is easily shown that the neutron, which has a mass comparable with that of the proton, should show patterns as illustrated in the top curve of Fig. 2. This occurs because, even though the mass is large, the interaction potential is very weak.

One should note that the energy is only a scaling factor in Eqs. (7) and (13), and, consequently, changing its value can only lead to a contraction or expansion of the θ scale, but not to a change in the characteristics of the angular variation of the intensity. From this observation it is easily understandable that the de Broglie wavelength cannot be the important characteristic length which characterizes the correspondence limit. A change in all the other variables, however, changes the ratio of θ_B to $\Delta\theta_B$ and should be expected to lead to different characteristics in the angular variation of the intensity.

The middle curves in Figs. 1 and 2 illustrate what occurs if the mass is increased to that of the positron and electron. The intensity for 100 and 200 electronic masses are illustrated in the bottom curves of Figs. 1 and 2. Let us first discuss Fig. 1, which represents positively charged particles. We note that the angular variation about the origin has changed considerably. The value at the origin has decreased markedly compared with the lower-mass case. For the positron, the angle where the intensity has achieved a value greater than unity occurs at about $2\theta_B$. As we remarked in our previous paper, however, the two-beam solution at this mass is still an adequate representation for the qualitative behavior of the intensity pattern. The structure beyond $2\theta_B$ resembles closely those in Fig. 1 (upper curve) and is associated with higher-order reflections.

[5] R. E. De Wames and W. F. Hall, Acta Cryst. **A24**, 206 (1968).

As we increase the mass to correspond to 100 and 200 electronic mass, the angular-intensity variations for these two cases are very nearly identical. Clearly, the Bragg angle has lost its significance to characterize the angular variation, since its value falls in the region where the intensity is flat. Furthermore, since these patterns are found to be nearly insensitive to changes in the mass, one immediately concludes that neither θ_B nor $\Delta\theta_B$ can be characteristic angles.

For this case, the two-beam theory loses meaning; this certainly is not surprising, since using a single reflection in the expansion of φ can only be justified if $\theta_B/\Delta\theta_B \gg 1$. This new behavior for the angular variation of the intensity, which is independent of the mass (and of $\hbar$), can tentatively be identified as the classical result. We see that its onset is governed not by the requirement $k_h\lambda \ll 1$, where λ is the de Broglie wavelength of the particle, but by

$$\begin{aligned}(\theta_B/\Delta\theta_B)^{1/2} &= \hbar k_h/2(mV_h)^{1/2}\\ &= k_h\lambda_p \ll 1,\end{aligned} \tag{14}$$

where the effective wavelength λ_p defined above tends to zero with increasing mass or potential strength, but is independent of particle energy.

It now becomes very interesting to compare the predictions of the simplified classical model of Lindhard with the predictions of the dynamical theory in the high-mass limit. To this end, we have studied empirically the dependence of the angular half-width on several parameters and found that for a screened Coulomb potential the dependence on the planar separation $d_p = 2\pi/k_h$ and the range of the potential Λ^{-1} appears to be much closer to

$$\begin{aligned}\theta_p &\propto (\theta_B\Delta\theta_B)^{1/2},\\ &\propto (V_h/2E)^{1/2},\\ &\propto \left(\frac{2\pi Ze^2\rho}{E(k_h^2+\Lambda^2)}\exp[-\tfrac{1}{2}(k_h^2\langle x^2\rangle)]\right)^{1/2},\end{aligned} \tag{15}$$

than to Lindhard's critical angle[1]

$$\theta_c \propto [y(0)/E]^{1/2} \propto (2\pi Ze^2\rho d_p/E\Lambda)^{1/2}, \tag{16}$$

where $\langle x^2\rangle$ is the mean-square displacement of the atom, ρ is the particle density, and y is the average planar potential defined by Lindhard. The point here is not in the actual values but in the functional dependence on the above parameters.

In Fig. 2, the angular variation for the intensity of negatively charged particles is illustrated. For the electron, θ_W indicates the position of the wings as calculated from the two-beam theory. We note that, as in the case for positively charged particles, the angular variation of the intensity at large mass becomes insensitive to further changes in the mass. However, the electron behavior can hardly be considered to be in the high-mass limit. In particular, the intensity about zero angle, apart from having different values, exhibits quite a different character. We also note that the value of the intensity at zero angle, in contrast to the behavior for positively charged particles, is still mass-dependent at $100m_e$. This behavior, however, appears to be restricted to a very narrow angular region.

To conclude this section, let us state again: It is certainly evident that for masses including those of electrons and positrons, the calculation of the angular intensity must be carried out quantum mechanically, if one is interested in anything beyond gross phenomenology.

Furthermore, for light-mass particles, the angular variation of the intensity is properly accounted for by θ_W, which is an explicit function of the mass of the particle. On the other hand, for the screened Coulomb potential whose characteristic parameters are those appropriate for the copper lattice, the angular variation of the intensity is found to be nearly mass-independent when the mass of the incident particle exceeds the electronic mass by about two orders of magnitude. In Sec. IV, this behavior is studied in more detail by calculating the value of the intensity for zero angle of incidence.

IV. POTENTIAL DEPENDENCE OF EMITTED INTENSITY

A. Planar Effects

In this section, we evaluate the intensity for zero angle of incidence for the planar geometry of Sec. III. Several potentials are considered in order to illustrate some of the difficulties in defining a classical limit for the intensity.

For the screened Coulomb potential and for reasonable values of the mean-square displacement, the intensity seems to tend towards a limiting value, as shown in Figs. 3 and 4. For zero mass, as can be shown from the two-wave solution, the intensity starts at unity. As the mass of the incident particle is increased, the probability density on the nucleus decreases for positively charged particles and increases for negatively charged particles. Figure 3 shows a smooth behavior

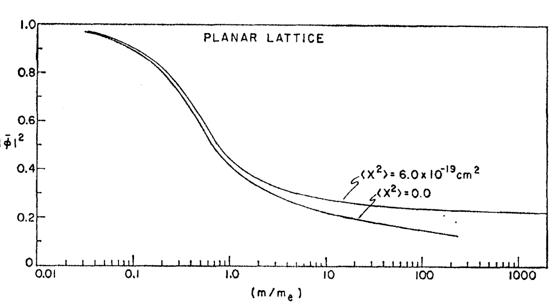

FIG. 3. Mass dependence of the intensity for zero angle of incidence and positive interaction potential.

for the positively charged particle, tending towards a limiting value quite sensitive to the value of $\langle x^2 \rangle$. It is interesting to note that the heavier-mass particle is more sensitive to the potential, in that a change in $\langle x^2 \rangle$ leads to large changes in the intensity, in contrast to the behavior in the low-mass region. The actual potential of interaction when $\langle x^2 \rangle \neq 0$ is a convolution of the screened Coulomb potential with the Debye-Waller factor.

Figure 4, which is the intensity for the negatively charged particle, fails to show limiting behavior through 200 electronic masses; however, as mentioned above, this mass dependence seems to be contained within a very small angular region.

A more interesting property of the curve is the fact that, in contrast to the positively charged particle, it is less smooth. In fact, between 1 and 10 electronic masses the intensity exhibits considerable structure. This, however, when viewed as a result of changing the mass, is of only academic value. But one should remember that for zero angle of incidence the probability density is symmetric in the mass and the atomic number Z of the host crystal, so that the curves in Figs. 3 and 4 can be viewed as a variation in Z for fixed mass. The point labeled 1 electronic mass corresponds to $Z=29$.

From the discussion presented so far one could conclude that, for the screened Coulomb potential with constants appropriate for the various elements, the angular variation of the intensity appears to converge towards a limit independent of the mass or of $\hbar$. One might be tempted at this stage to generalize this result to other potentials, and, in fact, simply require that the strength of the potential and the mass of the incident particle be large enough to ensure a limiting form for the angular variation of the intensity.

To illustrate the danger in generalizing numerical results, we have plotted (in Fig. 5) the intensity at zero angle of incidence for a variety of potentials. The

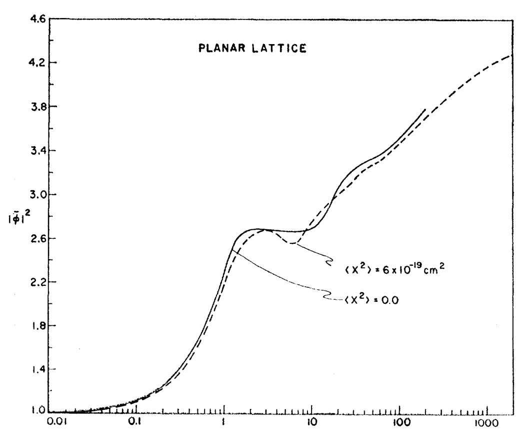

FIG. 4. Mass dependence of the intensity for zero angle of incidence and negative interaction potential.

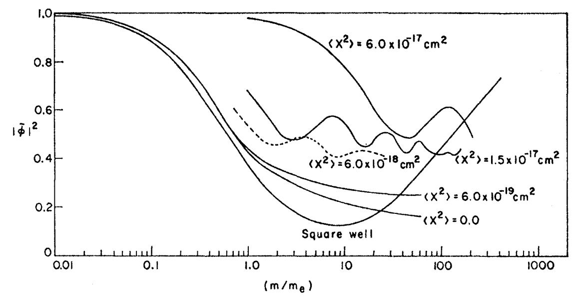

FIG. 5. Mass dependence of the intensity at zero angle of incidence for a variety of positive interaction potentials.

simplest of these is the square-well potential, which, in fact, has been used for calculations in channeling phenomena. This potential shows peculiar anomalies: The first distinct behavior is the upswing of the intensity towards unity for positively charged particles of sufficiently large mass. Our present method of calculation cannot determine the behavior for masses beyond that of the proton. However, by using a different mathematical procedure,[6] it is possible to establish the high-mass limit for zero angle of incidence. It turns out that for this potential there is no limiting value for the intensity in the sense discussed previously. In fact, the intensity tends toward a periodic function of the mass of the incident particle. The angular region over which these anomalies occur represents, for masses much beyond that of the proton, a fair fraction of the critical angle, so that averaging the intensity over a small angular region will not remove these effects.

In an attempt to identify which property of the potential is responsible for these anomalies, we have studied a variety of potentials which were constructed by a convolution of the screened Coulomb potential and the Debye-Waller factor. These potentials, for large mean-square displacement, have in common with the square-well potential a large region about the nuclei where the variation in the potential is small. As indicated in Fig. 5, we again obtain oscillatory behavior, but of quite different character. These characteristics will be discussed more fully in a future paper.[6] The point that we wish to make here is that using simple criteria to establish a correspondence limit can lead to erroneous results. Furthermore, the use of the square well to make calculations for charged particles leads to predictions which are inconsistent with results obtained for more realistic potentials.

B. String Effects

When the incident wave vector is taken to lie parallel to a principal lattice direction in the simple cube, the crystal is effectively a square array of continuous "strings" parallel to $\mathbf{k}_0$. As mentioned above, in this circumstance, advantage can be taken of the reflection

[6] G. W. Lehman and R. E. De Wames, Bull. Am. Phys. Soc. **13**, 438 (1968).

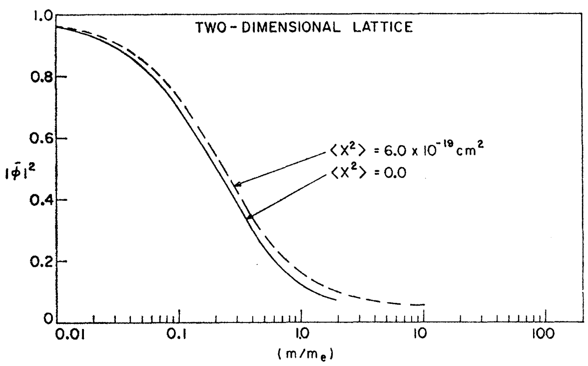

FIG. 6. Mass dependence of the intensity for the two-dimensional lattice at zero angle of incidence with positive interaction potential.

and rotation symmetry of the scattering geometry to obtain the intensity for fairly large particle mass, which would normally require the diagonalization of large-order matrices.

The primary purpose served by these calculations is to show that there is no intrinsic difference in the emitted intensity obtained in a string direction; one does not reach the classical limit any more quickly than in the planar case. The results of our calculations are illustrated in Figs. 6 and 7.

Comparing Figs. 3 and 6, we note that for the string case the intensity near the positron mass is decreased by about a factor of 2. The two curves, however, are very similar in shape. The percentage change due to thermal vibrations seems to be more pronounced for the string case.

The intensity for the negatively charged particle is illustrated in Fig. 7. Here again, just as in the planar case, we note structure in the mass dependence. The magnitude of the intensity, however, is much greater than in the planar case.

To summarize our numerical studies of the potential dependence of the intensity, it seems reasonable to say that for realistic potentials the quantum-mechanical calculation is tending toward a limit which is independent of the mass of the particle. This limiting value depends upon the mean-square displacement $\langle x^2 \rangle$ of the crystal atom. It is entirely possible that when $\langle x^2 \rangle = 0$, the intensity is tending toward zero as $m \to \infty$, which is believed to be the classical result for the emission problem. However, as was indicated in Fig. 3, at a mass corresponding to that of the proton, the intensity cannot yet be said to have achieved this limit.

CONCLUSIONS

By solving the emission problem quantum mechanically, we have been able to investigate the mass dependence, at constant energy, of the emitted intensity. Classically, there should be no such dependence, so that our results provide a useful measure of the applicability of the classical theory to emission experiments.

The case of electron and positron emission deserves special attention in this regard, since these particles are frequently used as experimental probes in crystals. To use a classical theory for emission when it is well known that the transmission patterns are controlled by Bragg angles and Bragg widths is simply inconsistent. Moreover, our calculations show (cf. Fig. 2) that, although there is a superficial similarity, the emission patterns differ from the classical limit in half-width and in intensity by factors of up to 4, with pronounced differences in shape.

The dramatic mass dependence that we have illustrated in this paper should dispose, once and for all, of the often-voiced notion that the emitted-intensity pattern for charged particles, regardless of mass, consists of a broad, dominant classical envelope on top of which is superposed small, detailed structure due to the (quantum-mechanical) Bragg resonances. The emission patterns at $\frac{1}{10}$ electronic mass no longer possess any resemblance to the classical envelope; the value of the intensity at $\theta = 0$ is unity, regardless of the sign of the charge, and departure from this value occurs only in the immediate vicinity of Bragg angles.

Even the more plausible suggestion that for a given scattering potential the emitted intensity tends everywhere toward a classical limit as the mass increases is called into doubt by the results that we obtain at

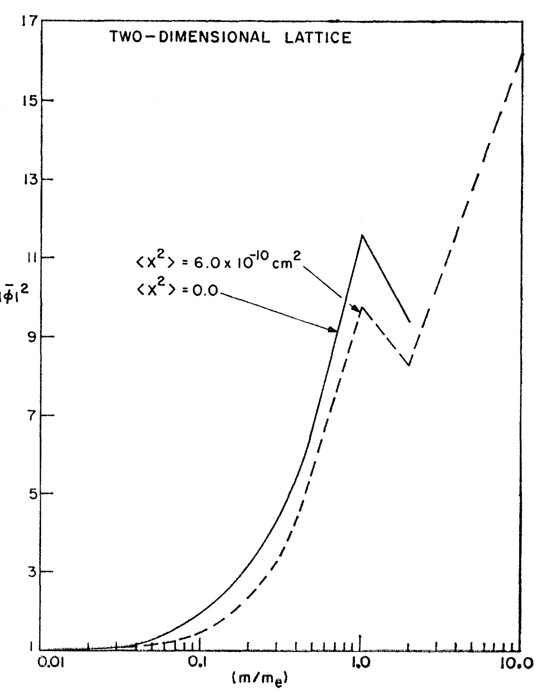

FIG. 7. Mass dependence of the intensity for the two-dimensional lattice at zero angle of incidence and negative interaction potential.

zero angle for the square well or for the screened Coulomb potential at sufficiently large mean-square displacement. While these anomalies are of limited angular extent, their existence points up the difficulties inherent in defining when a classical limit can be used for this problem.

Finally, let us point out that much of the current controversy over the adequacy of the classical description results from the inadequacy of the energy and angular resolution achieved in the experiments to date. As we pass to the use of more nearly monoenergetic particles (e.g., K-conversion electrons) and better angular resolution, the gross differences between the classical predictions for electrons and positrons and their actual behavior will become detectable.

APPENDIX

We denote by Γ_1 the point in the Brillouin zone (BZ) where $k_{0x}=k_{0y}=0$. If we are considering cubic crystals, then the group of the wave number k is a subgroup of the full cubic group and is denoted by C_{4V}. The amplitude $\varphi(\mathbf{r})$ must then transform like the Γ_1 irreducible representation of C_{4V}. We can therefore expand $\varphi(\mathbf{r})$ in terms of these symmetrized plane waves and derive equations for the coefficients in the expansion. The resulting equations, as we shall show, are very similar to those derived previously. However, matrices of lower order can be used to obtain the same accuracy in the calculation.

We write

$$\varphi^{\Gamma_1}(\mathbf{r})=e^{ikz}\sum_{n_1\geq n_2} A_{\mathrm{n}}\psi_{\mathrm{n}}^{\Gamma_1}(\mathbf{r}), \tag{A1}$$

where $\mathbf{n}=(n_1, n_2)$, n_1 and n_2 are Miller indices, k is the magnitude of the wave vector in the medium and needs to be determined from Eq. (1), and $\psi_{\mathrm{n}}^{\Gamma_1}$ is a linear combination of plane waves constructed in the following way:

$$\psi_{\mathrm{n}}^{\Gamma_1}=[(\sqrt{8})(\sum_S \delta_{\mathbf{k}_{\mathrm{n}},S\mathbf{k}_{\mathrm{n}}})^{1/2}]^{-1}\sum_R \exp(iR\mathbf{k}_{\mathrm{n}}\cdot\mathbf{r}), \tag{A2}$$

where R represents the elements of the group C_{4V} and δ is Kronecker δ. The above basis functions have been normalized so that

$$\int \psi_{\mathrm{n}}^{\Gamma_1}(\mathbf{r})\psi_{\mathrm{n}}^{\Gamma_1}(\mathbf{r})\,d\mathbf{r}=\mathbf{\Omega}, \tag{A3}$$

where Ω is the volume of the unit cell.

Now, using Eqs. (A1), (A2), and (7), we obtain for the A's

$$[(\hbar^2/2m)(k^2+k_{\mathrm{n}}^2)-E]A_{\mathrm{n}} + \sum_{n_1'\geq n_2'} \frac{A_{\mathrm{n}'}\sum^R U(\mathbf{k}_{\mathrm{n}}-R\mathbf{k}_{\mathrm{n}'})}{[(\sum_t \delta_{\mathbf{k}_{\mathrm{n}'},\, t\mathbf{k}_{\mathrm{n}}})(\sum_R \delta_{\mathbf{k}_{\mathrm{n}},\, R\mathbf{k}_{\mathrm{n}}})]^{1/2}}=0, \tag{A4}$$

where

$$U(\mathbf{k}_{\mathrm{n}}-R\mathbf{k}_{\mathrm{n}'})=(1/\mathbf{\Omega})\int \exp[i(\mathbf{k}_{\mathrm{n}}-R\mathbf{k}_{\mathrm{n}'})\cdot\mathbf{r}]U(\mathbf{r})\,d\mathbf{r}. \tag{A5}$$

Equation (A4) is very similar to Eq. (7), which we developed for the u_{h}'s. The important point to note is the reduction in the sum over that obtained without the use of group theory. We now proceed as before to obtain the wave functions inside the crystal by matching to the incoming plane wave at the entrance surface. This enables us to write

$$\varphi^{\Gamma_1}(\mathbf{r})=\sum_j A_{0j}\sum_R\sum_{n_1\geq n_2} A_{\mathrm{n}}{}^j\frac{\exp[i(k^{(j)}\mathbf{K}+R\mathbf{k}_{\mathrm{n}})\cdot\mathbf{r}]}{(\sqrt{8})(\sum_t \delta_{\mathbf{k}_{\mathrm{n}},t\mathbf{k}_{\mathrm{n}}})^{1/2}}, \tag{A6}$$

where $\mathbf{K}$ is a unit vector in the z direction.

To obtain the wave function at the nucleus, $\mathbf{r}$ is simply equated to a lattice point. In Eq. (A6), the exponent through the term k makes the intensity oscillate as a function of the thickness through the sample. However, if this thickness is greater than the extinction distance, the oscillations are very fast and, after averaging over a finite interval Δt, give zero contribution to the probability density. We define this as the envelope, which simply is

$$|\varphi^{\Gamma_1}|^2_{\mathrm{env}}=(\sqrt{8})\sum_j |A_{0j}|^2[\sum_{n_1\geq n_2} A_{\mathrm{n},j}/(\sum_t \delta_{\mathbf{k}_{\mathrm{n}},t\mathbf{k}_{\mathrm{n}}})^{1/2}]^2. \tag{A7}$$

This function represents the probability density at the nucleus averaged over a small thickness interval Δt at a finite distance in the crystal. The A's occurring in Eq. (A7) are obtained by solving Eqs. (A4). The sum over j runs over all the roots of the secular equation (A4). The normalization condition for the A's follows from Eq. (A3) and is given by

$$\sum_{n_1\geq n_2} |A_{\mathrm{n}}|^2=1.0. \tag{A8}$$